Anal. Chem. **1997,** *69,* 3731−3740

Nondisturbing and Stable SERS-Active Substrates with Increased Contribution of Long-Range Component of Raman Enhancement Created by High-Temperature Annealing of Thick Metal Films

Alexei Feofanov, Anatoli Ianoul,[†] Evgeniy Kryukov, Sergei Maskevich,[‡] Gennady Vasiliuk,[‡] Leonid Kivach,[‡] and Igor Nabiev*[,†]

Optical Spectroscopy Division, Shemyakin and Ovchinnikov Institute of Bioorganic Chemistry, Russian Academy of Sciences, 117871 Moscow, Russia

High-temperature annealing of thick silver films (TSFs) deposited onto a smooth dielectric substrate leads to high-order self-organization of metal clusters on the film surface. A comparative atomic force microscopic (AFM) analysis of "as-deposited" and annealed TSFs (aTSFs) shows that uniform ellipsoidal roughness ∼41 × 25 nm in lateral cross section and ∼45 nm in height results after annealing. These metal clusters are mutually oriented so that the main lateral axes of the ellipsoids are nearly parallel. UV−visible data demonstrate a ∼300 nm hypsocromic shift of the bands corresponding to the collective surface plasmon modes. Additionally, a new (∼350 nm) band related to the normal component of the plasmon oscillations appears after annealing. This band was found to be strongly angle-dependent for p-polarized light. The aTSFs appeared extremely time- and organic solvent-stable versus as-deposited films. The aTSFs were found to be nondisturbing surface-enhanced Raman scattering (SERS)-active substrates in the application to studies of complexation of crown ether styryl dyes with metal ions. A pronounced SERS signal of the analyte rhodamine 6G was observed with aTSFs, even when the analyte was separated from the silver surface with five Langmuir−Blodgett monolayers of stearic acid. At the same time, depositing only a monolayer of stearic acid on the as-deposited film completely suppressed the SERS signal of the analyte. Finally, the self-assembling of Ag clusters on the surface of the aTSF, stimulated by the high-temperature annealing, results in the creation of a time- and organic solvent-stable SERS substrate with nanometer-scale quasi-periodical roughness, and this substrate exhibits an increased contribution of the electromagnetic component to the overall Raman enhancement.

Surface-enhanced Raman scattering (SERS)-active substrates prepared by silver evaporation onto glass or silica slides are widely used in spectroscopic applications.[1−5] A number of studies to clarify the dependence of the films' properties on their preparation have been performed.[6−9] As in the cases of roughened electrodes,[5] metal sols,[10] or self-assembled colloidal films,[11−14] the surface structures were found to depend on a number of experimental factors. The quality of the glass substrate, deposition rate and temperature, deposition geometry, and postdeposition annealing were found to be important for producing high-quality SERS-active metal films.[7] These conditions are easy to control, and reproducible SERS-active films can be prepared by maintaining a consistent experimental procedure.[2] On comparing UV−visible, SERS, and atomic force microscopy (AFM) data, the optical and SERS properties of the films were found to correlate with their morphologies.[6]

As visualized by AFM, annealed Ag films undergo a change in the surface morphology. AFM imaging of the "as-deposited" and annealed island films shows that the silver granules typically increase in size and interparticle distances increase as the annealing proceeds.[6] As the surface morphology changes, the corresponding extinction spectra undergo a hypsochromic shift of absorption maxima, a decrease in optical density, and a narrowing of the surface plasmon extinction bands.

The main obstacles of the analytical use of Ag films in SERS applications include (1) a fast degradation of the Raman enhancing

* Author to whom correspondence should be addressed. Fax: +33-326826001. E-mail: igor.nabiev@univ-reims.fr.

[†]Current address: UFR de Pharmacie, Université de Reims Champagne-Ardenne, 51 rue Cognacq Jay, 51100 Reims, France.

[‡]Current address: Department of Physics, Yanka Kupala State Grodno University, 69900 Grodno, Belarus.

(1) Meier, M.; Wokaun, A.; Vo-Dinh, T. *Anal. Chim. Acta* **1986**, *181*, 139−143.
(2) Ni, F.; Cotton, T. M. *Anal. Chem.* **1986**, *58*, 3159−3163.
(3) Davies, J. P.; Pachuta, S. J.; Cooks, R. G.; Weaver, M. J. *Anal. Chem.* **1986**, *58*, 1290−1299.
(4) Moody, R. L.; Vo-Dinh, T.; Fletcher, W. H. *Appl. Spectrosc.* **1987**, *41*, 966−969.
(5) Nabiev, I. R.; Sokolov, K. V.; Manfait, M. *Biomolecular Spectroscopy*; Wiley: London, 1993; Chapter 7, pp 267−338.
(6) Van Duyne, R. P.; Hulteen, J. C.; Treichel, D. A. *J. Chem. Phys.* **1993**, *99*, 2101−2114.
(7) Semin, D. J.; Rowlen, K. L. *Anal. Chem.* **1994**, *66*, 4324−4331.
(8) Schlegel, V. L.; Cotton, T. M. *Anal. Chem.* **1991**, *63*, 241−247.
(9) Sokolov, K.; Khodorchenko, P.; Petukhov, A.; Nabiev, I.; Chumanov, G.; Cotton, T. *Appl. Spectrosc.* **1993**, *47*, 515−522.
(10) Kerker, M. *Acc. Chem. Res.* **1984**, *17*, 271−277
(11) Chumanov, G.; Sokolov, K.; Cotton, T. M. *J. Phys. Chem.* **1996**, *100*, 5166−5168.
(12) Chumanov, G.; Sokolov, K.; Gregory, B.; Cotton, M. *J. Phys. Chem.* **1995**, *99*, 9466−9471.
(13) Freeman, R. G.; Grabar, K. C.; Allison, K. J.; Bright, R. M.; Davis, J. A.; Guthrie, A. P.; Hommer, M. B.; Jackson, M. A.; Smith, P. C.; Walter, D. G.; Natan, M. J. *Science* **1995**, *267*, 1629−1632.
(14) Grabar, K. C.; Freeman, R. G.; Hommer, M. B.; Natan, M. J. *Anal. Chem.* **1995**, *67*, 735−743.

S0003-2700(97)00304-1 CCC: $14.00

properties due to oxidation of the silver clusters serving as adsorption sites for analyte (discussed below); (2) instability in organic solvents;[15] (3) "bio-incompatibility" of some film preparations, i.e., disturbance of the structure of adsorbed molecules and/or intramolecular or molecule−ligand interactions due to strong (often chemical) interactions between the molecules and the surface;[9,16] (4) a pronounced positive (in relation to the zero charge point of silver) charge of the surface of an as-deposited Ag film which hinders adsorption and, thereby, prohibits a SERS study of positively charged molecules;[17] and (5) a short-range (as compared with the length of a chemical bond) character of the Raman enhancement, unsuitable for studying some macromolecules, high molecular weight complexes, and cells.[9]

In this paper, we present a new type of SERS-active surfaces produced by high-temperature annealing of thick silver films (TSFs). These surfaces have been revealed to be extremely time-stable, almost insensitive to many organic solvents, and practically nondisturbing as applied to the studies of Mg^{2+} binding by the crown ether styryl dyes. The surface of the annealed thick silver films (aTSFs) has been found to carry a more negative charge and to exhibit an increased contribution of the electromagnetic component to the overall Raman enhancement in relation to that of as-deposited TSFs.

EXPERIMENTAL SECTION

Reagents. Ag powder, 5−8 mm, was used for preparation of Ag films (Aldrich, 99.99%). A compound with the electronic transition in the visible, rhodamine 6G (Rh6G, 98%), and a compound with the electronic transition in UV, pyridine (Pyr, 99%) were used as purchased (Sigma). UV spectroscopy grade ethanol, acetonitrile, methanol, and acetone (Fluka) were used as received. Concentrations of stock solutions of pyridine (H_2O) and Rh6G (acetonitrile or H_2O) were 0.1 and 10^{-6} M, respectively. All other chemicals were of analytical grade.

Photochromic crown ether dyes 2-[2-(2,3,5,6,8,9,11,12-octahydro-1,4,7,10,13-benzopentaoxacyclopentadecyn-16-yl)ethenyl]-3-(3-sulfopropyl)benzothiazolium betaine; 2-[2-(2,3,5,6,8,9,11,12-octahydro-1,4,7,10,13-benzopentaoxacyclopentadecyn-16-yl)ethenyl]-3-ethyl benzothiazolium perchlorate, and 2-methyl-3-ethylbenzothiazolium perchlorate were a gift from Semenov Institute of Chemical Physics (Moscow, Russia). 2,3,5,6,8,9,11,12-Octahydro-1,4,7,10,-13-benzopentaoxacyclopentadecyne was purchased from Merck. Acetonitrile solutions of the photochromic dyes were prepared and all experiments carried out under red light at room temperature. Acetonitrile was doubly distilled from P_2O_5 and CaH_2 to remove traces of water which disturb complexation of the photochromic dyes with metal cations. Magnesium perchlorate was dried under vacuum at 180 °C.

Apparatus. TSFs were fabricated with a VUP-5 vapor deposition system. The pressures in the diffusion pumped chamber were $<10^{-5}$ Torr. The deposition source was a tungsten boat filled with a Ag powder (2−5 mg). The film thickness and deposition rates were monitored with a photometric control as described[9] and with AFM. The AFM calibration of mass thickness was performed by masking half of the substrate and depositing silver over the unmasked half, as described by Van Duyne et al.[6] Then, the AFM tip was repetitively scanned over the boundary in order to calculate the average thickness of deposited silver film. To measure the resistivity of the films, two silver electrodes were deposited at the edges of the film surface.

A custom-built temperature-controlled aluminum block served as a substrate holder for thermal experiments. The substrate temperatures were measured with a calibrated thermocouple placed in direct contact with the substrate. A second thermocouple was positioned in the same plane and adjacent to the substrate to follow radiative heating changes during deposition.

Optical absorption spectra were measured with a Cary 209 double-beam UV−visible spectrophotometer.

SERS spectra were recorded with a single-channel Ramanor HG-2S spectrometer (Jobin Yvon) using an Ar^+ laser (Spectra-Physics, Model 164-03) and a Kr^+ laser (Karl Zeiss, Model ILK-120). The laser power was 50 mW (λ_{exc} = 647.1 nm), 5 mW (λ_{exc} = 457.9 nm), 15 mW (λ_{exc} = 488 nm), or 25 mW (λ_{exc} = 514.5 nm). Laser plasma lines were eliminated by sending the beam through a premonochromator (Anaspec 300S). The experimental conditions are specified in the figure legends. Typically, spectra were recorded in 150−1700 cm^{-1} range at 1 cm^{-1} increments with 1 s integration time as an average of 1−4 accumulations. All spectra were reproduced at least three times for different sample preparations. The characteristic spectral features discussed below were reproducible from one preparation to another and over multiple experiments.

The excitation profiles were measured with the 457.9, 476.5, 488.0, 496.5, and 514.5 nm lines of the Ar^+ laser and 568.2, 647.1, and 676.1 nm lines of the Kr^+ laser. The intensity of the 1008 cm^{-1} band of pyridine used for measurement of the profiles was reduced for the factor ν^4 and corrected for the monochromator−detector response and for laser power.

Mono- and multilayers of stearic acid were prepared with a NFT and Lauda (Germany) Langmuir−Blodgett troughs as follows. Stearic acid chloroform solution (6 μM) was deposited with a microsyringe (50 μL) on the surface of bidistilled water. The monolayers were transferred to a solid support at a pressure of 20 mN/m by the Langmuir−Blodgett technique. Each monolayer deposited on the solid support was carefully dried in air before the next was deposited. The observed transfer ratios for mono- and multilayer preparations were close to unity.

Procedures. *Slide Pretreatment.* Glass microscope and quartz slides were obtained from Fisher Scientific Inc. The cleaning procedure involved washing the slides in the chromium salt solution, followed by successive sonications in deionized water, ethanol, and acetone. The slides were dried at 120 °C for 20 min and cooled to room temperature before introduction into the vapor deposition system.

Silver Film Deposition. The slides were placed in the deposition unit ~12 cm above a tungsten boat that served as the heating source. The deposition rate was controlled by the current passed through a tungsten boat. Unless otherwise stated, a fixed deposition rate of 0.4 Å/s was used. The film thickness reported herein was ~140 Å. All films were manufactured at an Ag deposition angle of ~90° with the slide plane.

Annealing. Annealing of TSFs deposited on glass or quartz substrates was performed in the muffle heating system at four

(15) Feofanov, A.; Ianoul, A.; Oleinikov, V.; Gromov, S.; Fedorova, O.; Alfimov, M.; Nabiev, I. *J. Phys. Chem.* **1996**, *100*, 2154−2160.
(16) Otto, A.; Mrozek, I.; Grabhorn, H.; Akermann, W. *J. Phys., Condens. Matter* **1992**, *4*, 1143−1168.
(17) Maskevich, S. A.; Gachko, G. A.; Znevsky, G. V., Podtychenko, S. G. In *Proceedings of the XIV International Conference on Raman spectroscopy*; Yu, N.-T., Li, X.-Y., Eds.; Wiley: Chichester, UK, 1994; pp 644−645.

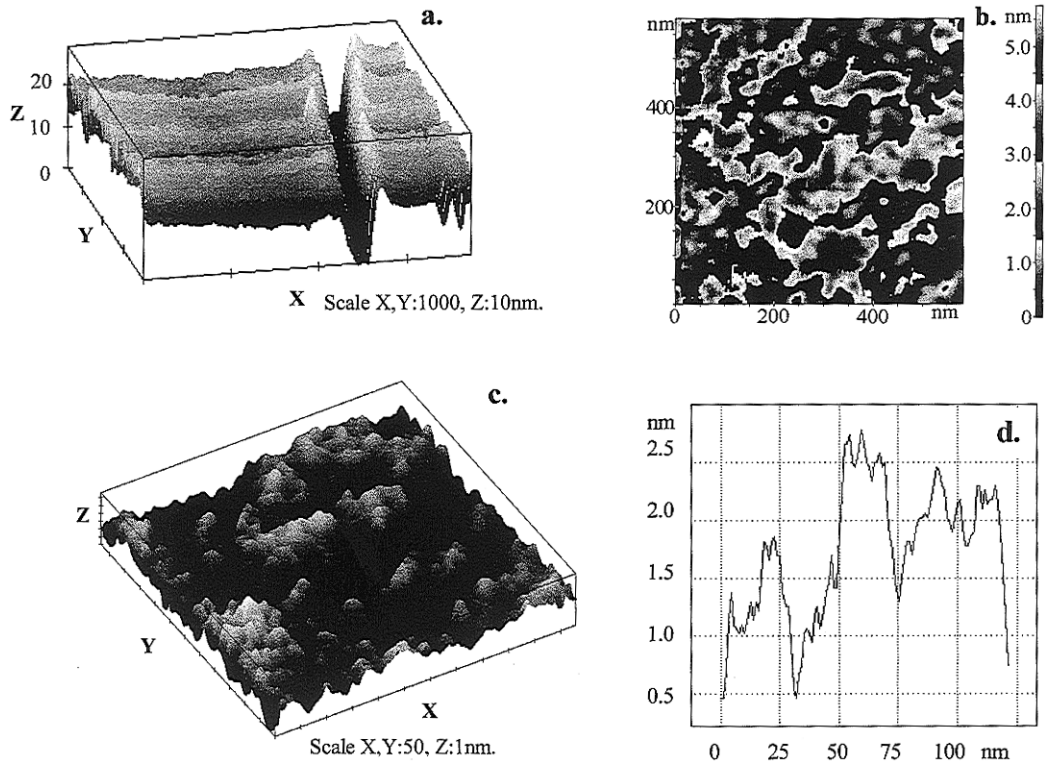

Figure 1. AFM images (a, b, c) and line profile (d) for the as-deposited TSFs. AFM resolutions: 10 (a), 2 (b), and 0.5 (c) nm.

stages for 6 min each: 125, 175, 225, and 350 °C. After each stage, the films were cooled to room temperature, and their extinction spectra were recorded. An effect of self-organization of the metal clusters on the surface of aTSFs was observed with AFM: the surface morphology of the aTSF was compared with the initial morphology of TSFs and with the morphology of TSFs deposited onto glass or quartz substrates preheated to 350 °C.

Characterization of Silver Films. AFM images were taken in air using a Nanotechnology P4-SPM AFM/STM microscope. The images reported here are raw, unfiltered data collected in the constant force mode (i.e., the tip−sample separation is adjusted to maintain a constant force equal to 15−25 nN) with a scan speed of 8 lines s^{-1}. A scan head with range of 7 μm × 7 μm was routinely used. Commercial Si_3N_4 cantilever tips (Park Scientific Instruments) with spring constants of ∼0.12 nm^{-1} were used. The tips were pyramidal in shape, with a cone angle of 70° and an effective radius of curvature at the tip of ∼40 nm.

Lateral sizes of the silver particles measured with AFM microscope were corrected for the effect of broadening due to the finite tip size. The correction was made according to the equation

$$Z = \sqrt{X(X + 2Y)}$$

where Z is the dimension of roughness as measured with the tip having a radius of curvature of Y nm, and X is the real dimension of roughness.

For the aTSFs, the distributions of lateral dimensions of silver particles (after correction for the tip-induced broadening), ratios of lateral dimensions of the particles, ratios of lateral sizes to the height of the particles, and mutual orientations of the particles are presented in the form of histograms. Average values and standard deviations were calculated for the parameters listed above.

Deposition of Samples. Four procedures were utilized for sample deposition onto the Ag films:

(i) The SERS-active surface was spotted with a 5 μL drop of the analyte in a volatile solvent (water, methanol, ethanol, propanol, or acetonitrile) and dried. SERS spectra were recorded immediately following the procedure.

(ii) One or several monolayers of stearic acid were deposited by the Langmuir−Blodgett method (see above), followed by coating with a drop of the analyte.

(iii) The monolayer of sample was deposited by the Langmuir−Blodgett method ("fatty" crown, see below).

(iv) A mountable thin (0.2 mm) quartz cell was filled with solution of analyte. The rear wall of the cell was substituted for the TSF plate.

RESULTS AND DISCUSSION

General Characteristics of the Surfaces of As-Deposited and Annealed TSFs. Figure 1 shows AFM images of as-deposited TSFs recorded at different resolutions. The thickness of the as-deposited films used for preparation of annealed films was ∼14 nm. An accurate measurement of the film thickness was obtained by the analysis of AFM images of the needle trace on the surface of the film (Figure 1a). The surface of the as-deposited film has a granulated structure and may be regarded as a surface with random roughness (Figure 1b,d). High-resolution AFM imaging reveals these granules to be silver clusters and their aggregates on the film surface. The roughness features of the film can be characterized by the lateral orthogonal size metrics, a and b, and the height of clusters or particles, c. The shape of the particle is estimated by the ratio (R) of the height (c) to the main lateral size (a) of the particle ($R = c/a$), as well as by the ratio (L) of the main lateral size (a) to the orthogonal lateral size (b) of the particle ($L = a/b$). The orientation of the particle

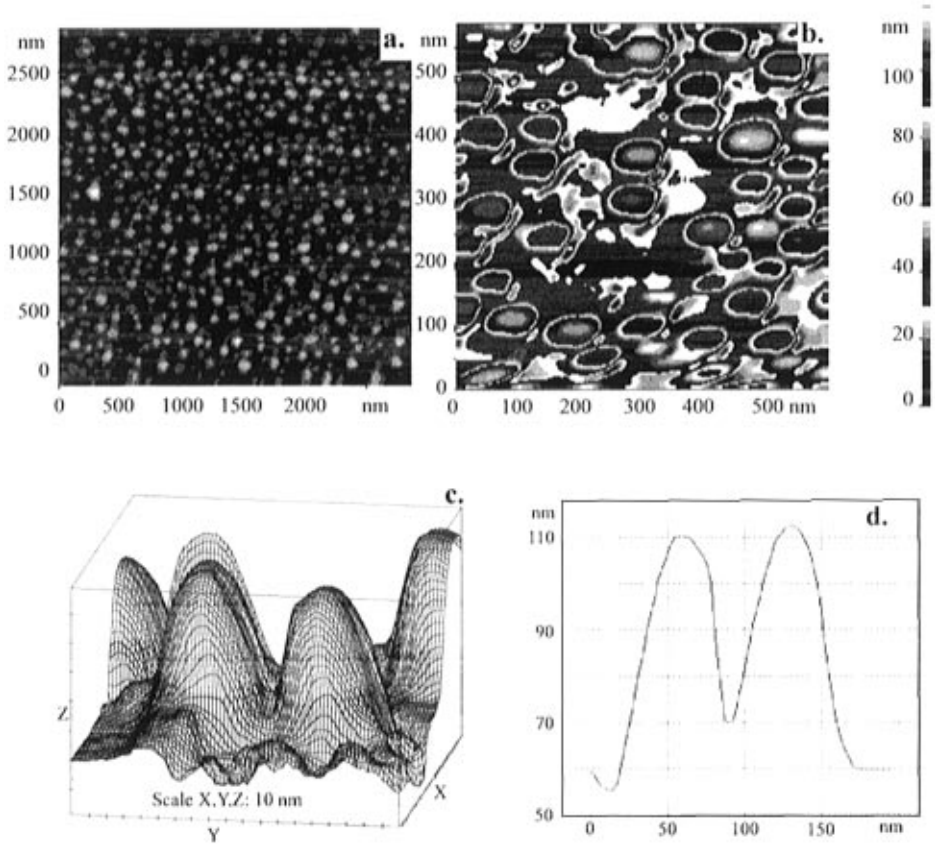

Figure 2. AFM images (a, b, c) and line profile (d) for aTSFs. AFM resolutions: 10 (a), 2 (b), and 0.5 (c) nm.

is characterized by the angle between the *a* axis of the particle and the *x* axis of the AFM scanning system. In terms of the electromagnetic mechanism of the SERS effect,[6] the particle shape (values of *R* and *L*) is considered to dominate in correlation between the regularity of roughness, optical properties, and SERS activity of a film. As is seen from the AFM images of the as-deposited TSFs, *a* and *b* vary randomly from 1 to more than 100 nm, whereas *c* (derived from the peaks in the AFM line profile data, Figure 1d) varies from 0.1 to 4 nm. Statistical analysis of the surface roughness gives an average *R* value of ~0.01−0.1. The AFM images presented here (Figure 1) resemble those of Van Duyne et al.[6] and Schlegel and Cotton[8] obtained at deposition rates of ~5 Å/s. It is necessary to note that the films used in our work are "continuous" (not "island"), and their roughness is due to the clusters and cluster aggregates on the silver surface (Figure 1).

Figure 2 shows AFM images of the annealed TSFs. The annealing dramatically changes the surface topology of TSFs. Two principal features of the aTSF surface should be stressed: (i) the annealing induces formation of highly regular island-type silver features with a demiellipsoidal form of the islands on a smooth quartz support and (ii) the annealing disassembles the silver clusters or their aggregates which are characteristics of the as-deposited film (compare Figures 1c,d and 2c,d).

Resistivity of ~2 mΩ × cm was found to be typical for the continuous as-deposited TSF of 14 nm mass thickness. This value significantly exceeds the rated resistivity of bulk Ag (1.6 μΩ-cm). It seems to be reasonable, because the defects of the film surface dramatically increase the resistivity when the ratio of surface area to the volume of silver film is rather high. The first stage of the annealing results in a 2-fold increase in the film resistivity. After the next annealing stages, the film's resistivity reaches values exceeding 0.1 MΩ-cm. Island-like structure of silver roughness and tremendous values of resistivity enable us to consider aTSFs as the island films. Being closely distributed, these demiellipsoidal islands may overlap one another (Figure 2b).

Statistical analysis of the lateral dimensions (*a* and *b*) of the islands (Figure 3a,b) revealed that the average values of *a* and *b* are 41 ± 22 nm and 25 ± 13 nm, respectively. Lateral cross sections of the islands are ellipses, and the average value of *L* is 1.7 ± 0.2 (Figure 3b). The main lateral axes *a* of the islands are parallel to one another, as can be seen from the histogram, which shows distribution of the angles between the a axes of the particles and the *x* axis of the AFM scanning system (Figure 3d). The average height of the islands is 45 ± 15 nm, and the average ratio *R* is 0.86 ± 0.45. Analysis of the histogram for the *R* value shows that the main fraction of the particles has height *c* nearly equal to either the *a* or *b* values (Figure 3c).

Although the TSFs used in our studies are "continuous", a wide variety of macrodefects may be found at their surfaces. High-temperature annealing of our as-deposited thick silver layer leads to dispersion of the layer into small, isolated regions at the expense of a breakup of the mainly continuous film. Annealing leads also to the diffusion of these small silver clusters into a self-assembly of isolated islands.

It is known that annealing changes the morphology of both the island silver films and the thick silver films. A self-organization of small (~5 nm) particles into bigger (more than 10 nm) islands was observed by Van Duyne et al.[6] at the 600 K annealing of the island silver films. Similar effects were described by Semin and

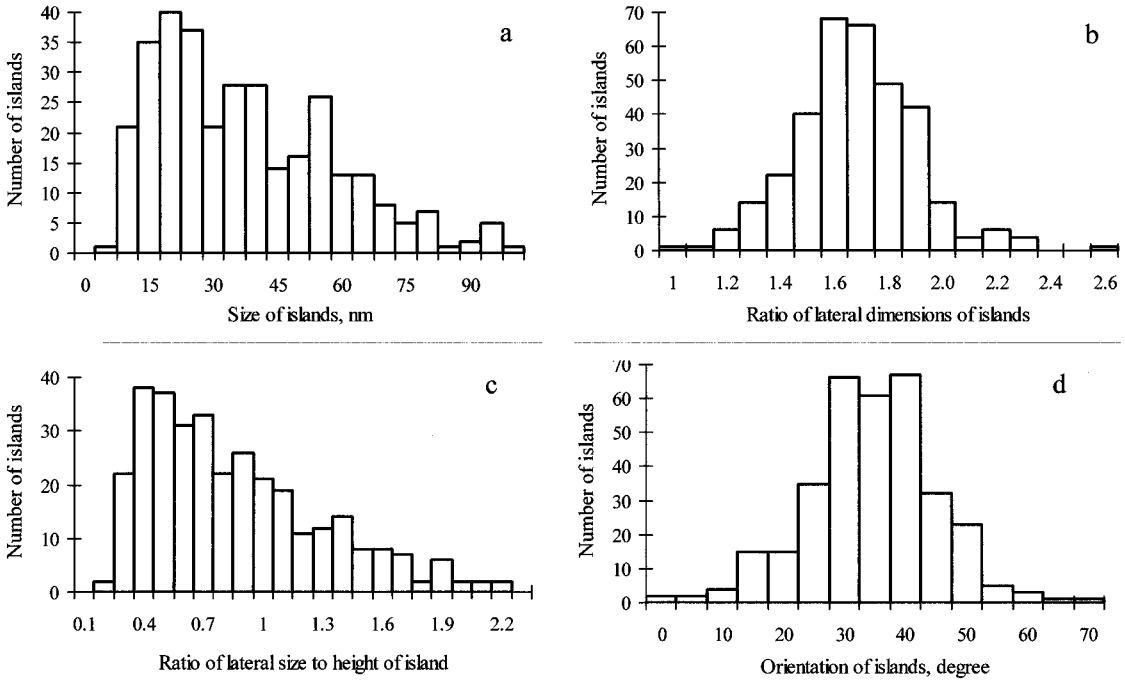

Figure 3. Distributions of the main lateral sizes *a* (a), ratios of lateral sizes *b/a* (b), and ratios of the height to the main lateral size *c/a* (c) of the silver islands on the aTSFs. Mutual orientation of the islands presented by the distribution of the angles between the a axis of the particle and the *x* axis of the AFM scanning system (d).

Rowlen[7] for silver deposited on hot quartz supports in vacuum. On the other hand, one-stage annealing of the thick (16 nm) film reported by Van Duyne et al.[6] leads to transformation of the large-scale roughness into small (40 nm) islands. This one-stage annealing mode does not produce self-organized uniform regular islands at the surface of a quartz support[6] as it does in our multistage annealing procedure. So, the processes of breakup of continuous film and the self-organization of silver clusters seem to be strongly dependent on the details of the annealing procedure and on the characteristics of the original as-deposited silver film used for annealing. In accordance with the theory of the SERS effect,[18] one may expect that the annealing-induced appearance of regular surface roughness on a 100 nm scale (Figure 2) increases a relative contribution of the electromagnetic component to the Raman enhancement due to excitation of the plasmon resonance within demiellipsoidal islands. This assumption was studied by comparison of both nonpolarized and polarized extinction spectra angle dependences (s- and p-polarization) for the as-deposited and annealed films.

Extinction Spectra of As-Deposited and Annealed TSFs. It is well-known that optical properties of silver island films depend on their mass thickness,[6] the rate of silver deposition,[7,8] the temperature of a solid support,[7] and the procedure of postdeposition annealing of the film.[6,7] Figure 4 shows nonpolarized extinction spectra of the TSFs at normal incidence for each of the four stages of the annealing procedure (see Experimental Section). The as-deposited TSFs (Figure 1a) exhibit a broad extinction band peaking at 700 nm (Figure 4, curve 1), characteristic of the spectra of TSFs published before.[9] The annealing induces dramatic changes in the extinction spectra. Extinction maxima of the TSFs annealed at 125−225 °C undergo a dramatic

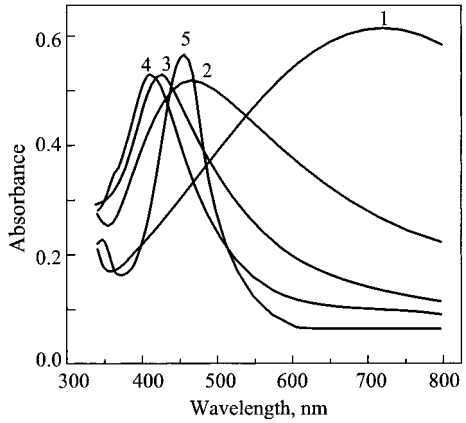

Figure 4. Extinction spectra of as-deposited TSF (1) and TSF annealed at 125 (2), 175 (3), 225 (4), and 350 °C (5) (see Experimental Section for details).

blue shift (from ~700 to 420 nm) and fall in intensity versus those of the as-deposited film (Figure 4). Also, the width of the extinction band decreases remarkably. The next stage of the annealing (up to 350 °C) leads to a further narrowing of the band, and the extinction increases slightly, while the extinction maximum shifts slightly back to 450 nm (Figure 4, curve 5). All the annealed films exhibit a loss of absorption in the deep red region. Further annealing and/or raising the temperature above 350 °C results in broadening and a moderate bathochromic shift of the TSF absorption spectra. An annealing-induced shift of the maximum to 445−460 nm and a change in the width of the extinction band depend on the initial absorption characteristics of the as-deposited film. A new extinction band at 350 nm (Figure 4, curve 4) also becomes prominent after annealing. This band is assigned to excitation of the in-plane plasmon resonance within regular uniform surface features.[10]

The appearance of blue-shifted extinction maxima has been previously reported for thermally annealed silver island films

(18) Fleischmann, M.; Hendra, P. J.; McQuillan, A. J. *Chem. Phys. Lett.* **1974**, *26*, 163−166.

deposited on rock salt[19] and on glass[20] substrates. The shifts were interpreted as thermally induced breakup of silver particles, so that new nucleation sites appear, resulting in formation of particles with increased height. Indeed, when red-shifted extinction maxima have been observed for annealed island films, the SEM and TEM micrographs have revealed that the particles in annealed films are larger in diameter than those of as-deposited films.[21 22] Increasing of particle size accompanied by the red-shift of extinction maxima was interpreted as being consistent with the electromagnetic theory. On the other hand, the shape factor of particles, *R*, was found to be the same before and after annealing.[22]

Obviously, there are two processes we have described after analysis of the AFM images of the TSFs that determine the behavior of extinction spectra in the course of annealing. First, the growth of quite big (~41 nm × 25 nm × 45 nm) islands appeared as a result of self-organization of the clusters and reorganization of a continuous part of the film. This process leads to ~10-fold increase of *R*, a main roughness parameter, and results in a blue-shifted extinction band. The second process is a significant increase in interparticle distances on the film surface. As a result, the particles become more isolated, and interparticle dipole−dipole interactions (a parameter determining the width of the extinction bands of TSFs[21]) are significantly reduced.

A slight bathochromic shift of the extinction maximum from 420 to 450 nm which occurs at the fourth stage of the annealing (Figure 4) may be explained by the tendency of the particles to acquire a homogeneous form (Figures 2 and 3). The island homogeneity of the aTSFs also suggests an appearance of a new absorption band at 350 nm due to excitation of the out-of-plane plasmon resonance.[23]

Absorption intensities of out-of-plane and in-plane plasmon components are sensitive to both polarization and the incidence angle of light. Figure 5 shows extinction spectra of as-deposited and annealed films at the different incidence angles of p- and s-polarized light. We observed a p-polarized light absorption to change dramatically with an angle of incidence. This fact may be explained in terms of possibility for p-polarized light to excite both out-of-plane and in-plane plasmon modes. As the angle increases, the excitation of the in-plane plasmon oscillations becomes less probable, whereas the out-of-plane oscillations are excited more efficiently. The angle dependence for p-polarized light is the most pronounced for aTSFs (exhibiting an island structure) as compared with the as-deposited films. At the angles of incidence of p-polarized light over 60°, the absorption at 350 nm dominates the absorption at 450 nm. It is noteworthy that the band of out-of-plane plasmon oscillations is much narrower than the in-plane plasmon band. Narrow bands of plasmon oscillations at ~350 nm are normally pronounced in systems of isolated uniform spheroidal particles.[21] Hence, the p-polarized light angular dependence is in close correlation with the AFM results on the film surfaces. Partial overlapping of the islands of the annealed TSFs to a greater extent influences the energy of

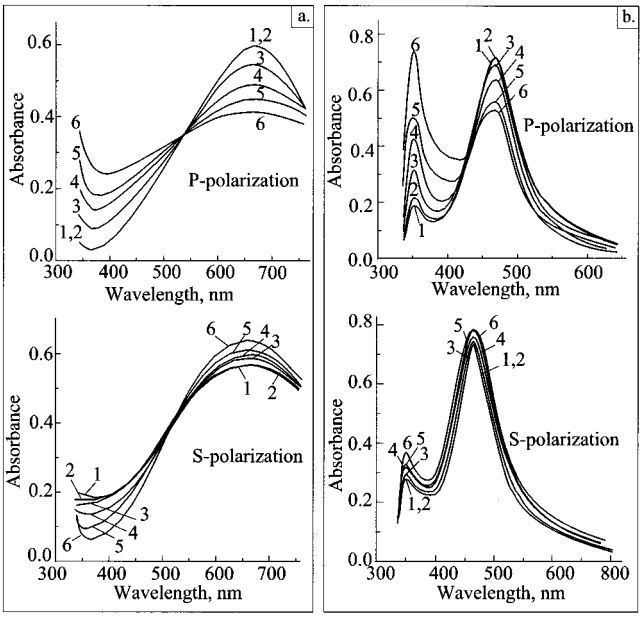

Figure 5. Extinction spectra of as-deposited (a) and annealed (b) TSFs recorded with s- or p-polarized light at incidence angles of 0° (1), 15° (2), 30° (3), 45° (4), 60° (5), and 70° (6).

in-plane plasmon vibrations and is a reason for the inhomogeneous broadening of the 450 nm absorption band.

As far as s-polarized light is concerned, only in-plane plasmon oscillations are driven. Therefore, the ratio of absorption intensities of the in-plane and out-of-plane plasmon excitations cannot depend on the incidence angle.[23] Both the as-deposited and the annealed films reveal some increase in absorption as a whole. This fact may be tentatively explained by an increase in the reflection coefficient.

One of the most important features of absorption of annealed films is the following. As the incidence angle for both s- and p-polarized light increases, a 4 nm blue-shift of the maximum at 450 nm (in-plane plasmon oscillations, Figure 5b) occurs. This effect, together with a remarkable growth of the narrow band at 350 nm with increasing incidence angle, should be regarded as a specific characteristic of the optical properties of the annealed films. It should be considered in the close relation to the appearance of collective phenomena in the system of uniform and regularly deposited spheroids.[24] The shift of the maximum at 450 nm suggests inhomogeneous broadening of this band, probably as a result of enhancement of multipole oscillations. These oscillations may be driven by the light with frequency polarization characteristics other than those used for excitation of dipole oscillations.[24]

Shifts of SERS Excitation Profile Due to Annealing. Apart from absorption shifts, the SERS excitation profile was also found to be modified after annealing. We recorded SERS spectra of pyridine adsorbed on the aTSFs and as-deposited TSFs with different excitation wavelengths. The intensity of the pyridine band at 1008 cm^{-1} was used for monitoring SERS-active properties of the films. As can be seen from Figure 6, the maximum of the excitation profile of the aTSFs (λ_{max} ~480 nm) is downshifted as compared to that of the as-deposited TSF (λ_{max} ~570 nm), and the width of the profile is decreased after annealing. This may

(19) McCarthy, S. L. *J. Vac. Sci. Technol.* **1976**, *13*, 135−138.
(20) Aussenegg, F. R.; Leitner, A.; Lippitsch, M. E.; Reinisch, H.; Riegler, M. *Surf. Sci.* **1987**, *189/190*, 935−945.
(21) Royer, P.; Goudonnet, J. P.; Warmack, R. J.; Ferrell, T. L. *Phys. Rev. B* **1987**, *35*, 3753−3756.
(22) Royer, P.; Bijeon, J. L.; Goudonnet, J. P.; Iganaki, R.; Arakawa, E. T. *Surf. Sci.* **1989**, *217*, 384−389.
(23) Aravind, P. K.; Nitzan, A.; Metiu, H. *Surf. Sci.* **1981**, *110*, 189−204.
(24) Ritchie, G.; Burstein, E.; Stephens, R. B. *J. Opt. Soc. Am. B* **1985**, *2*, 544−551.

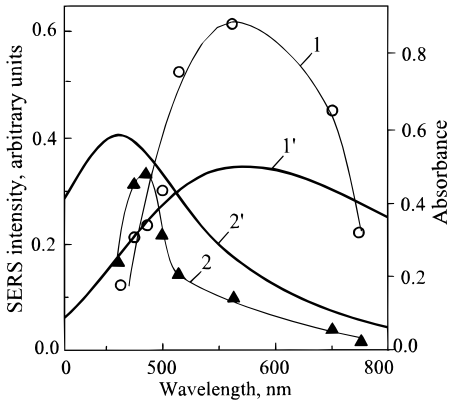

Figure 6. SERS excitation profiles of pyridine on as-deposited (1) and annealed (2) TSFs and extinction spectra of the corresponding as-deposited (1′) and annealed (2′) TSFs.

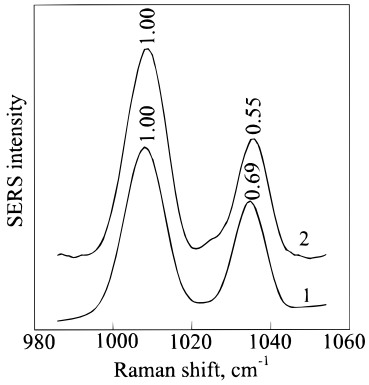

Figure 7. SERS spectra of pyridine, adsorbed on the surface of as-deposited (1) and annealed (2) TSF. Pyridine concentration, 0.05 M in 0.1 M KCl aqueous solution; λ_{ex} = 514.5 nm; laser power, 50 mW.

be due to a dominance of the electromagnetic mechanism of the Raman enhancement on the aTSFs. As a result, the correlation of a SERS excitation profile maximum with an extinction maximum of the film was observed.

Change in the Surface Potential of TSFs Induced by Annealing. As is known, the surface potential of a SERS-active substrate is often responsible for adsorption and other properties of an analyte on the surface and, thereby, determines applicability of the method to a particular object.[25] The SERS spectrum of pyridine was demonstrated to depend on a surface potential: varying potential induces reorientation of the molecule, and, thereby, a change in relative SERS intensities of the 1008 and 1034 cm^{-1} pyridine bands is observed.[25] So, in order to compare surface potentials of the aTSFs and TSFs, SERS spectra of pyridine were recorded. Figure 7 shows that a characteristic of the aTSFs is a decrease in the ratio of intensities of 1008/1034 cm^{-1} bands from ~0.69 to 0.55. These values correspond to a decrease in surface potential of a roughened silver electrode in the electrochemical cell from ~−0.5 to −0.6 V. Hence, after annealing, the potential of the surface of TSF becomes more negative and closer to the zero charge point of silver.

Time and Organic Solvents Stability of the Raman-Enhancing Properties of Annealed TSFs. Among the properties determining analytical applications, stability of TSF is rather important. Two aspects of stability should be considered: the stability of Raman-enhancing properties of the substrates as a function of time and their stability to organic solvents.

(25) Weits, D. A.; Moskovits, M.; Creighton, J. A. In *Chemistry and Structure at Interfaces*; Hall, R. B., Ellis, A. B., Eds.; VCH: Deerfield Beach, FL, 1986; pp 197−243.

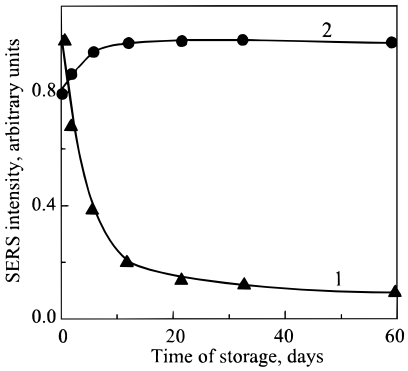

Figure 8. Time stability of SERS-active properties of as-deposited (1) and annealed (2) TSFs tested with a 5 μL drop of a 10^{-6} M water solution of Rh6G.

Table 1. Comparative Stability of TSFs with Different Organic Solvents

	absorbance A/A_0,[a] rel. un. (%)		SERS I/I_0,[b] rel. un. (%)	
solvent	TSF	aTSF	TSF	aTSF
acetonitrile	<10	30	25	95
methanol	<10	67	<5	70
propanol	74	84	28	30
DMSO	<10	70		

[a] Optical density before (A_0) and after (A) treatment with solvent. [b] R6G SERS intensity before (I_0) and after (I) treatment with solvent.

To compare the stability of the aTSFs and as-deposited TSFs with time, we followed SERS spectra of Rh6G adsorbed on freshly prepared films 1, 6, 12, 21, 32, and 60 days after preparation. Figure 8 presents the results of this study. A more than 2-fold decrease in the Raman-enhancing properties of the as-deposited TSFs 6 days after preparation contrasts with the almost unchanged and even increased Raman enhancement of analyte on the aTSFs. Furthermore, the Raman-enhancing properties of the aTSFs were found to persist virtually for 60 days.

Table 1 shows the changes of the Raman-enhancing and optical properties of TSFs in different organic solvents. We measured absorption spectra of the films prior to and after 10 min of exposure to a solvent. The same procedure was used for SERS measurements, and the analyte, Rh6G, was deposited on the films prior to and after the treatment. The ratios of A/A_0 (optical densities of the films after (A) and before (A_0) treating with a solvent) and I/I_0 (normalized SERS intensities of the analyte after (I) and before (I_0) the exposure) were used in order to estimate the effect of an organic solvent on the film. The results presented in Table 1 imply higher solvent stability of the aTSFs versus the as-deposited TSFs. Despite a sufficient degradation of the Raman enhancement of the aTSFs in propanol, these films remain almost unperturbed in acetonitrile and methanol. The acetonitrile stability data are particularly interesting, since a rather small change in SERS intensity occurs with the large change in the aTSF optical density. Our recent results show that treatment with the aceto-

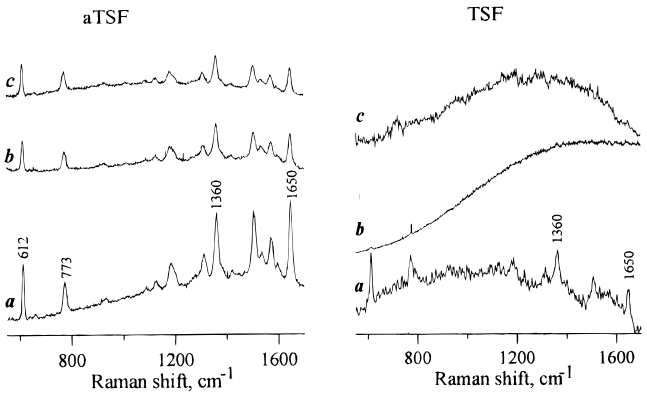

Figure 9. SERS intensity of Rh6G spaced from the surface of as-deposited or annealed aTSFs with 0 (a), 1 (b), or 5 (c) Langmuir–Blodgett monolayers of stearic acid. A 5 μL drop of a 10^{-6} M solution of Rh6G was deposited as an analyte.

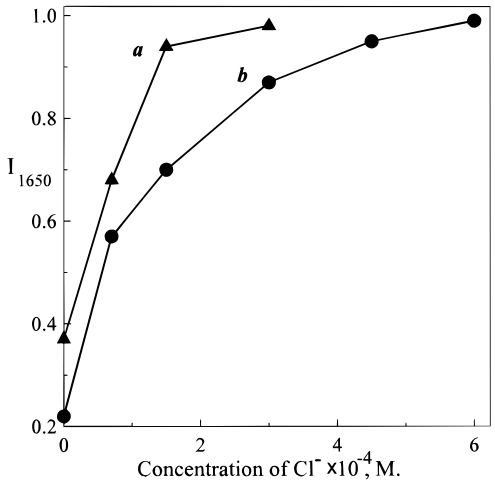

Figure 10. Dependence of the relative intensity of the 1650 cm^{-1} SERS band of Rh6G on the concentration of Cl^- anions in solution. The SERS spectra were recorded on the annealed (a) and as-deposited (b) films. A 5 μL drop of a 10^{-6} M water solution of Rh6G was deposited as an analyte.

nitrile modifies the morphology of the aTSF.[26] This modification is responsible for both the large change in the aTSF optical density and the surprisingly little loss of the SERS intensity.

Long-Range Component of Raman Enhancement Induced by High-Temperature Annealing of TSF. In order to find out relative contributions of short-range (chemical) or more long-range (electromagnetic) components of the Raman enhancement on the as-deposited TSFs and aTSFs, the SERS spectra of Rh6G adsorbed on a bare surface and Rh6G separated from the silver surface by one and five monolayers of stearic acid were obtained (Figure 9). The SERS signal of Rh6G on the surface of the aTSFs appeared ~10 times more intense than that of Rh6G on the as-deposited TSFs. The intensity of the SERS spectra of Rh6G adsorbed on the aTSFs shows a moderate decrease on going from none to five monolayers of stearic acid. On the other hand, depositing a single monolayer of stearic acid on the surface of TSFs results in a total disappearance of the SERS signal of Rh6G (Figure 9). This points out the considerable contribution of the long-range electromagnetic component to the surface-induced enhancement of Raman signal for aTSFs, but not for as-deposited TSFs. Indeed, the molecular monolayers often have defects, and some molecules of analyte can penetrate through to the metal surface. In this sense, monolayer studies may fail to show long-range enhancement. However, once an additional marker exists that the major pool of molecules is separated from the bare silver surface, such investigation appears fairly reliable.

In our case, at least two evidences exist that the major fraction of Rh6G molecules adsorbed over the monolayers is separated from the bare silver. The first is a progressing change of the SERS spectrum of Rh6G when separated from the SERS-active surface of aTSF. In particular, the $I(773\ cm^{-1})/I(1650\ cm^{-1})$ ratio alters from 0.4 (bare silver) to 0.9 (five monolayers). Remarkably, the latter is the closest to the value observed for a resonance Raman spectrum of Rh6G in solution. The second evidence includes an absence of any SERS spectrum of Rh6G adsorbed on as-deposited TSF covered with a monolayer of stearic acid. It shows that the number of defects of monolayer(s) is very low and/or that an ability of Rh6G molecules to penetrate through the monolayer and to adsorb directly at the silver surface is negligible.

Assuming that the quality of the monolayers of stearic acid and penetration ability of Rh6G are very similar for both aTSFs and as-deposited TSFs, we finally conclude that our data strongly support long-range electromagnetic field enhancement for the aTSFs.

As was shown by Hildebrandt and Stockburger, two different kinds of adsorption sites exist on the surface of the SERS-active substrates.[27] One kind is unspecific, shows a high surface coverage, and corresponds to the induction of the "electromagnetic" component of Raman enhancement. The second kind of sites is observed only in the presence of anions: the sites are extremely specific and show low surface coverage. This second enhancement factor was ascribed to the local "chemical" mechanism of the SERS effect, which is related to formation of a Rh6G adatom (or cluster)–anion surface complex.[27] In order to evaluate the relative contribution of specific and nonspecific sites to the overall surface-induced enhancement of Raman signal, an effect of Cl anions on the SERS spectra of Rh6G has been studied for the as-deposited and annealed TSFs. We measured SERS spectra of Rh6G adsorbed on the as-deposited and annealed TSFs in the presence of increasing concentrations of Cl^- (Figure 10). Both substrates reveal the extra enhancement of the SERS signal as the anions are added, indicating formation of anion-activated sites on the surface. In the case of the aTSFs, the anion-induced surface complexes, however, are saturated at relatively small amounts of Cl^- compared to the as-deposited films (Figure 10). It indicates a lesser number of anion-activated sites on the surface of the aTSFs as compared to the as-deposited films. This fact implies that an enhancement associated with anion-induced adsorption sites—though present to some degree on the aTSF—becomes probably less important for the SERS effect after the annealing.

Although the data on activation of specific adsorption sites cannot provide complete evidence for reduced chemical enhancement on the aTSF, the major point is, however, that, having a fewer specific adsorption sites (anion-activated sites), the aTSF still exhibits profound enhancement properties.

(26) Maskevich S., Vasilyuk, G.; Sveklo, I.; Nabiev, I. In *Proceedings of the XV International Conference on Raman Spectroscopy*; Asher, S. A., Stein, P. B., Eds.; Wiley: Chichester, UK, 1996; pp 630–631.

(27) Hildebrandt, P.; Stockburger, M. *J. Phys. Chem.* **1984**, *88*, 5935–5944.

Crown Ether Styryl Dyes: Interactions with Mg As Probed by SERS on aTSFs. Probably the most important issue of application of SERS-active substrates in studies of intramolecular and molecule−ligand interactions concerns the so-called "biocompatibility" of the substrates (in terms of their "nondisruptivity" of the analyte's function). Since chemisorption necessarily involves chemical interactions between the adsorbed molecules and the surface, such an interaction would very likely perturb an analyte's structure. As is shown in the present work, annealing of TSFs induces self-organization of islands on a 100 nm scale and disappearance of the smaller Ag clusters and aggregates, which are the main source of the chemisorption sites for adsorbed molecules. Moreover, Langmuir−Blodgett/SERS measurements with Rh6G showed an increased contribution of the electromagnetic component to the overall Raman enhancement for the aTSFs versus the as-deposited TSFs.

We decided to test "nondisturbity" of the as-deposited and the annealed TSFs for the analyte's function in order to set the grounds for the studies of molecular and molecule−ligand interactions. For this, we investigated the process of binding of magnesium ions by some derivatives of crown ether styryl dyes (CESDs) adsorbed on the as-deposited and annealed TSFs. 2-[2-(2,3,5,6,8,9,11,12)-Octahydro-1,4,7,10,13-benzopentaoxacyclopentadecyn-16-yl)ethenyl]-3-(3-sulfopropyl)benzothiazolium betaine is a particular representative of photoresponsive CESDs. UV−visible and fluorescence spectroscopy studies of its photoisomerization and complexation with alkaline earth metal cations have revealed light- and cation-dependent changes in conformation, intermolecular interactions, and stoichiometry of metal−ligand complexes.[28]

Recently, we presented Raman and SERS spectra of some CESDs, their molecular fragments, and their complexes with Mg^{2+} cations.[15,29] The preliminary assignments of the SERS bands were made, and the characteristic spectral changes induced by complexation with Mg^{2+} cations were described. In first attempts, we failed to study CESDs by SERS with as-deposited TSFs and silver island films due to the extremely low stability of the films in acetonitrile. On the other hand, the aTSFs were found to be stable in this solvent (Table 1), and SERS spectra of CESDs may be readily recorded (Figure 11). Detection limits for CESDs were found to be $\sim 10^{-7}$ M when using aTSFs. The SERS spectrum of a free CESD on the aTSFs (Figure 11a) coincides with that obtained by us earlier with the use of a roughened electrode in an open-circuit electrochemical cell.[15,29]

The difficulty of independent control of the influence of a silver (or, in general, metallic) surface on a biomolecular structure concerns with the lack of "surface-enhanced" methods other than SERS spectroscopy. Discriminating a signal of molecules located in the vicinity of a surface is difficult due to interference from a strong background signal from the molecules in the bulk when detected by traditional (normally nonsurface-enhanced) methods of control.[5] Hence, it is necessary to use SERS spectroscopy itself to trace molecular structure in the vicinity of the metal surface

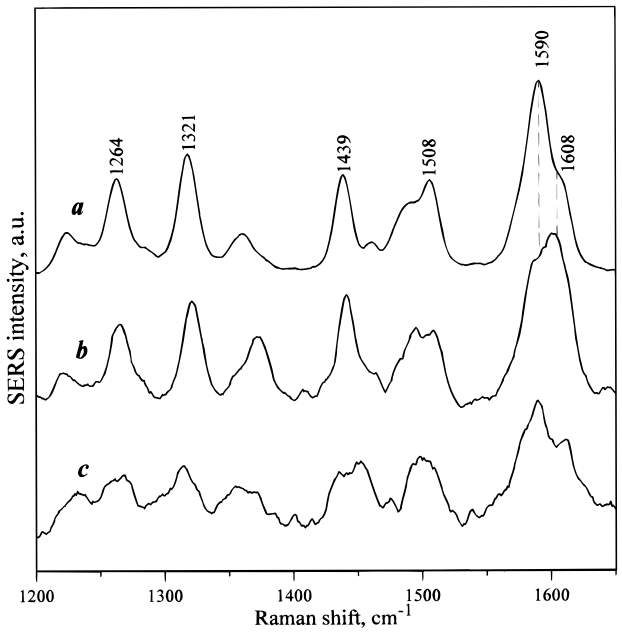

Figure 11. SERS spectra of benzothiazolium crown ether dyes: 2-[2-(2,3,5,6,8,9,11,12)-octahydro-1,4,7,10,13-benzopentaoxacyclopentadecen-16-yl)ethenyl]-3-(3-sulfopropyl)benzothiazolium betaine (a), its complex with Mg^{2+} (b), and 2-[2-(2,3,5,6,8,9,11,12,14,15-decahydro-1,4,7,10,13,16-benzohexaoxacyclooctadecyn-19-yl)ethenyl]-5-methoxy-3-octadecylbenzothiazolium perchlorate (c). All compounds are adsorbed on the aTSFs. $\lambda_{exc} = 457.9$ nm. Laser power, 3 mW. (a, b) Concentration of the dye in acetonitrile, 10 μM; mass quantity of the sampled molecules, $\sim 10^{-13}$ M; $[Mg^{2+}] = 1$ mM. (c) A single monolayer of the lipophilic compound deposited on the surface of the aTSF by the Langmuir−Blodgett technique.

by comparison of the corresponding Raman (or resonance Raman) and SERS spectra. Recently,[30] we applied this approach to the studies of mitoxantrone, a highly potent anticancer drug currently used in clinical trials of non-Hodgkin's lymphomas, acute myeloid leukemias, and advanced breast cancer. The objective of the study was to evaluate the influence of the surface of a silver hydrosol on the molecular interactions within drug−DNA complexes. SERS and preresonance Raman spectra were found to be nearly identical both in the frequencies and in the relative intensities of the bands. Moreover, interactions between the drug and DNA induced identical effects in the preresonance Raman, SERS, and FT-SERS spectra of the drugs. The data demonstrated applicability of SERS on the hydrosol for the analysis of drug (at least mitoxantrone)−DNA interactions under conditions preserving the structure of the complexes. In contrast to the drug−DNA complexes, the hydrosol was found to be nonsuitable for studying the cation binding properties of the CESDs.[15]

The aTSFs appeared as nondisturbing SERS-active substrates when applied to the studies of complexation of CESDs with metal ions. The pattern of the Mg^{2+} binding by CESD deposited on the surface of the aTSF was the same as that in solution (Figure 11b). Moreover, the CESD−Mg^{2+} binding constants measured independently by spectrophotometric and SERS (on the aTSF) titrations were found to be equal (manuscript in preparation). As far as the sensitivity is concerned, using the aTSF allows detection of a SERS signal even of a single monolayer of the lipophilic ("fatty") derivative of a CESD (Figure 11c). In terms of mass

(28) Barzykin, A. V.; Fox, M. A.; Ushakov, E. N.; Stanislavsky, O. B.; Gromov, S. P.; Fedorova, O. A.; Alfimov, M. V. *J. Am. Chem. Soc.* **1992**, *114*, 6381−6385.

(29) Feofanov, A.; Ianoul, A.; Gromov, S.; Fedorova, O.; Alfimov, M.; Nabiev, I. *J. Phys. Chem*., in press.

(30) Nabiev, I.; Baranov, A.; Chourpa, I.; Beljebbar, A.; Sockalingum, G.; Manfait, M. *J. Phys. Chem*. **1995**, *99*, 1608−1613.

quantity, $\sim 10^{-13}$ M concentration of the analyte was sufficient to elicit the spectrum.

CONCLUSIONS

Annealing of TSFs leads to high-order self-organization of metal clusters on the Ag film surface. Annealed TSFs are SERS-active substrates exhibiting superior time and organic solvent stability. The optical properties of these substrates could easily be monitored by UV−visible, and their surface morphology was scrutinized by AFM. The highly regular self-organized surface of the aTSF provides a preferential contribution of the "electromagnetic" (relatively long-ranged) component of the Raman cross section enhancement. The aTSFs were shown to be a nondisturbing SERS-active substrate when applied to the study of binding of magnesium ions by the crown ether styryl dyes. Finally, these substrates offer advantages combining "bio-compatibility", stability, and long-ranging enhancement, all making these substrates extremely promising in applications for the studies of macromolecules and high molecular weight supramolecular complexes.

ACKNOWLEDGMENT

This research was supported by Grant No. 1379 from ARC (France) and in part by NATO Grant HTECH.CRR961365 and by a grant from the Russian Foundation for Basic Research.

Received for review March 19, 1997. Accepted June 17, 1997.[⊗]

AC970304C

[⊗] Abstract published in *Advance ACS Abstracts,* August 1, 1997.